Supporting Information

ZrB_2 as an earth-abundant metal diboride catalyst for electroreduction of dinitrogen to ammonia

Qingqing Li, Yonghua Cheng, Xiaotian Li, Yali Guo, Ke Chu*

School of Materials Science and Engineering, Lanzhou Jiaotong University, Lanzhou 730070, China

*Corresponding author. E-mail address: chukelut@163.com (K. Chu)

Experimental Section

Synthesis of ZrB_2 nanocubes

All the chemicals are of analytical grade and used as received. The ZrB_2 nanocubes were prepared by a simple molten-salt method based on a reported method with a slight modification[1]. In brief, 1 mmol of $ZrCl_4$ and 2 mmol of MgB_2 were vacuum-sealed into a quartz tube, which was then transferred into a furnace. The tube was firstly heated from room temperature to 200 ^{o}C with a heating rate of 5 ^{o}C min^{-1} and kept for 2 h. Subsequently, the temperature was further increased to 900 ^{o}C with a heating rate of 3 ^{o}C min^{-1} and kept for another 5 h. After cooling down to room temperature, we got the final ZrB_2 nanocubes.

Electrochemical experiments

Electrochemical measurements were carried out on a CHI-760E electrochemical workstation by means of a conventional three-electrode cell. The catalyst dropped on carbon cloth (CC) was used as the working electrode, Ag/AgCl (saturated KCl) electrode was used as the reference electrode, and graphite rod was used as the counter electrode. All potentials were referenced to reversible hydrogen electrode (RHE) by following equation: E_{RHE} (V)=$E_{Ag/AgCl}$+0.197+0.059×pH. The CC substrate was pretreated by soaking it in 0.5 M H_2SO_4 for 12 h, and then washed with deionized water several times and dried at 60 ^{o}C for 24 h. To prepare working electrode, 1 mg of samples was dispersed in 100 μL of ethyl alcohol/Nafion (1:19 v/v) hybrid solutions and ultrasonically dispersed to form a homogeneous ink. Then, 20 μL of ink was dropped onto the 1×1 cm^2 CC substrate (mass loading: 0.2 mg cm^{-2}), and dried naturally. The NRR test was performed on an H-type two-compartment electrochemical cell separated by a Nafion 211 membrane [2-4]. The Nafion membrane was pretreated by boiling it in 5% H_2O_2 solution for 1 h, 0.5 M H_2SO_4 for 1 h and deionized water for 1 h in turn. Prior to electrolysis, the feeding gases were purified through 0.05 M H_2SO_4 solution to remove any possible contaminants (NH_3 and NO_x). During each electrolysis, ultra-high-purity N_2 gas (99.999%) was continuously purged into the cathodic chamber at a flow rate of 20 mL min^{-1}. After

each NRR electrolysis, the produced NH_3 and possible N_2H_4 were quantitatively determined by the indophenol blue method[5], and approach of Watt and Chrisp[6], respectively.

Determination of N_2H_4

5 mL of electrolyte was removed from the electrochemical reaction vessel. The 330 mL of color reagent containing 300 mL of ethyl alcohol, 5.99 g of $C_9H_{11}NO$ and 30 mL of HCl were prepared, and 5 mL of color reagent was added into the electrolyte. After stirring for 10 min, the UV-Vis absorption spectrum was measured and the concentration-absorbance curves were calibrated by the standard N_2H_4 solution with a series of concentrations.

Determination of NH_3

4 mL of electrolyte was removed from the electrochemical reaction vessel. Then 50 μL of solution containing NaOH (0.75 M) and NaClO (ρ_{Cl}=~4), 500 μL of solution containing 0.32 M NaOH, 0.4 M $C_7H_6O_3$, and 50 μL of $C_5FeN_6Na_2O$ solution (1 wt%) were respectively added into the electrolyte. After standing for 2 h, the UV-Vis absorption spectrum was measured and the concentration-absorbance curves were calibrated by the standard NH_4Cl solution with a series of concentrations.

$$\mathrm{NH_3\ yield}\ (\mu\mathrm{g\ h^{-1}\ mg_{cat.}^{-1}}) = \frac{c_{\mathrm{NH_3}} \times V}{t \times m} \tag{1}$$

Faradaic efficiency was calculated by the following equation:

$$\text{Faradaic efficiency (\%)} = \frac{3 \times F \times c_{\mathrm{NH_3}} \times V}{17 \times Q} \times 100\% \tag{2}$$

where c_{NH3} (μg mL^{-1}) is the measured NH_3 concentration, V (mL) is the volume of the electrolyte, t (h) is the reduction time and m (mg) is the mass loading of the catalyst on CC. F (96500 C mol^{-1}) is the Faraday constant, Q (C) is the quantity of applied electricity.

Characterizations

Transmission electron microscopy (TEM), high-resolution transmission electron microscopy (HRTEM) and energy dispersive X-ray (EDX) were carried out on a Tecnai G^2 F20 microscope. X-ray diffraction (XRD) pattern was recorded on a

Rigaku D/max 2400 diffractometer. X-ray photoelectron spectroscopy (XPS) was conducted on a PHI 5702 spectrometer. The UV-vis absorbance measurements were recorded on a MAPADA P5 spectrophotometer. ^{1}H nuclear magnetic resonance (NMR) measurements were performed on a 500 MHz Bruker superconducting-magnet NMR spectrometer. Prior to NMR measurements, all the feeding gases were respectively purified by an acid trap (0.05 M H_2SO_4) to eliminate the potential NO_x and NH_3 contaminants [7].

Calculation details

Spin-polarized density functional theory (DFT) calculations were carried out using a Cambridge sequential total energy package (CASTEP). The Perdew–Burke–Ernzerhof (PBE) generalized gradient approximation (GGA) functional was used for the exchange-correlation potential [8]. The DFT-D correction method was considered for van der Waals forces. During the geometry optimization, the convergence tolerance was set to be 2.0×10^{-5} eV for energy and 0.05 eV $Å^{-1}$ for force. The Brillouin zone was sampled in a 4×4×1 mesh. The electron wave functions were expanded using plane waves with a cutoff energy of 400 eV. The ZrB_2 (001) was modeled by a 2×2 supercell, and a vacuum region of 15 Å was used to separate adjacent slabs.

The Gibbs free energy (ΔG, 298 K) of reaction steps is calculated by [9]:

$$\Delta G = \Delta E + \Delta ZPE - T\Delta S \quad (3)$$

where ΔE is the adsorption energy, ΔZPE is the zero point energy difference and $T\Delta S$ is the entropy difference between the gas phase and adsorbed state. The entropies of free gases were acquired from the NIST database.

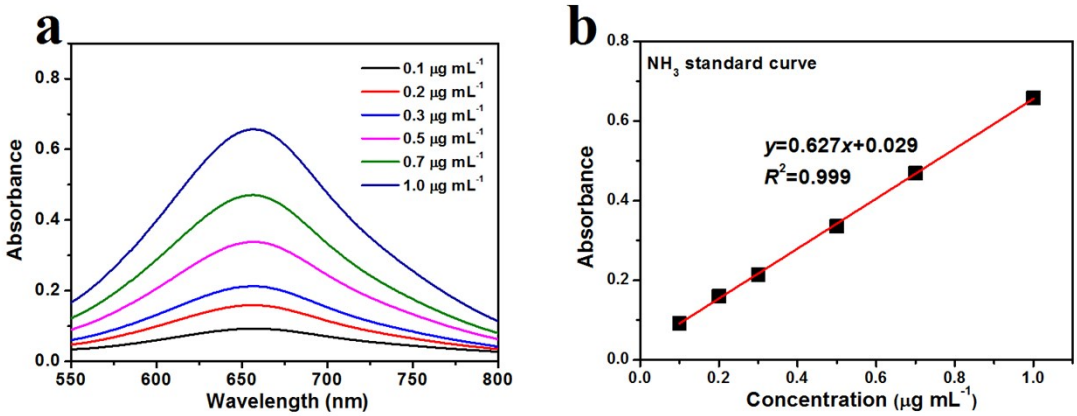

Fig. S1. (a) UV-vis absorption spectra of indophenol assays with NH_4Cl after incubated for 2 h at ambient conditions. (b) Calibration curve used for calculation of NH_3 concentrations.

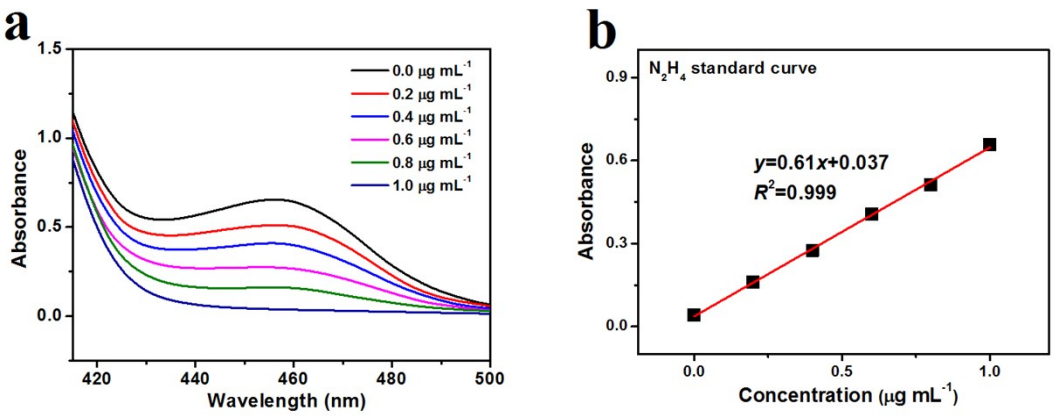

Fig. S2. (a) UV-vis absorption spectra of N_2H_4 assays after incubated for 20 min at ambient conditions. (b) Calibration curve used for calculation of N_2H_4 concentrations.

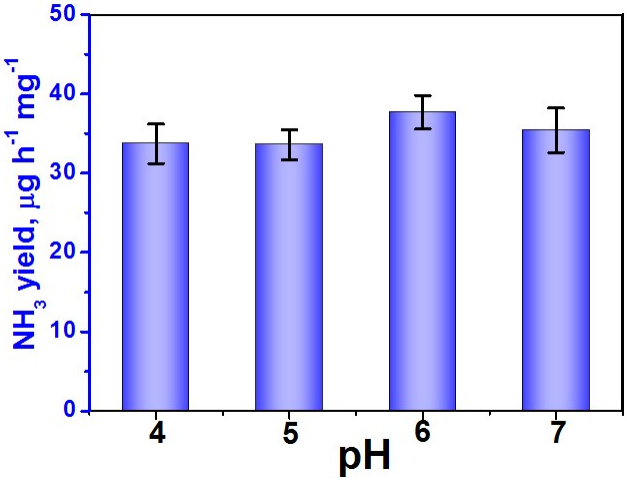

Fig. S3. pH effect of 0.5 M $LiClO_4$ on the NH_3 yield of ZrB_2 NCs

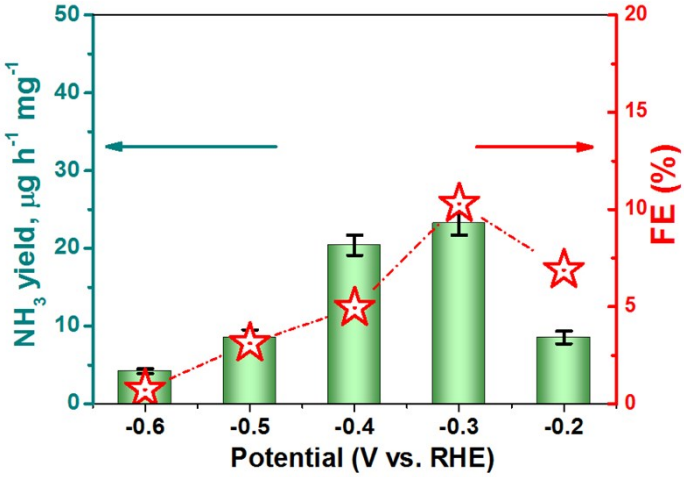

Fig. S4. NH_3 yields and FEs of ZrB_2 NCs in 0.1 M Na_2SO_4 electrolyte at various potentials.

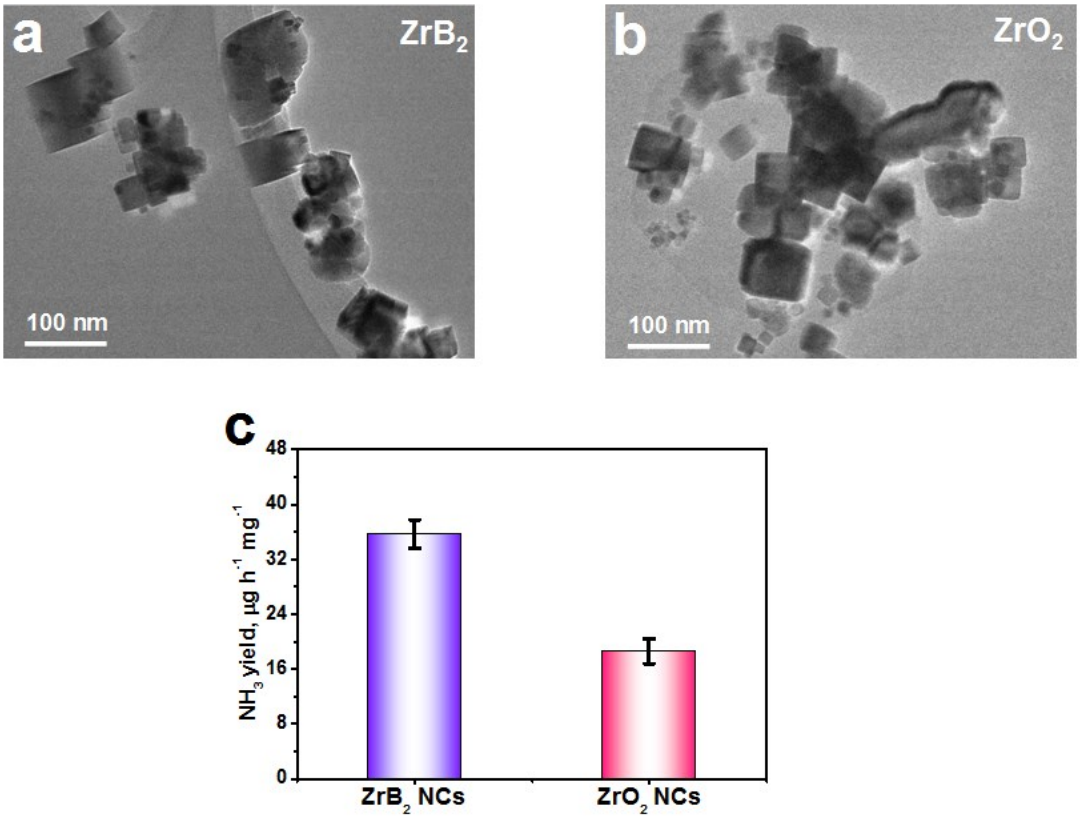

Fig. S5. (a, b) Morphologies of ZrB_2 NCs and ZrO_2 NCs and (c) their NH_3 yields at -0.3 V. ZrO_2 NCs were prepared by annealing ZrB_2 NCs in a muffle furnace at 300 °C for 2 h under air atmosphere.

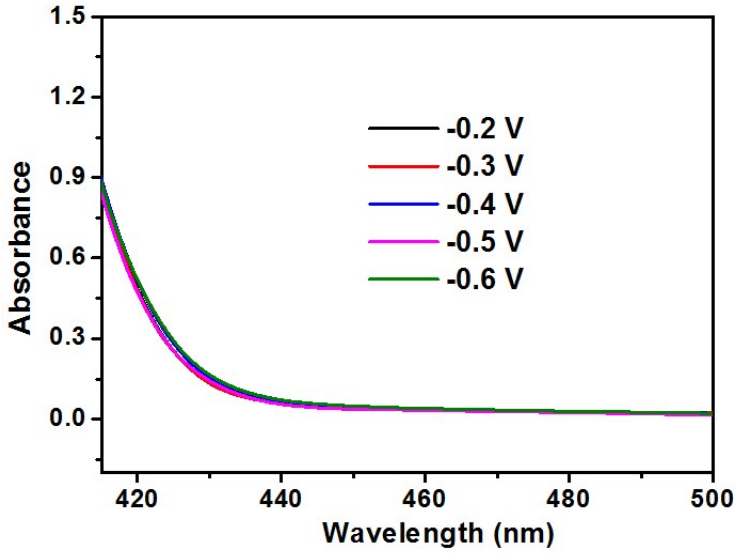

Fig. S6. UV-vis spectra of the electrolytes (stained with the chemical indicator based on the method of Watt and Chrisp) after 2 h of electrolysis on ZrB_2 NCs at various potentials.

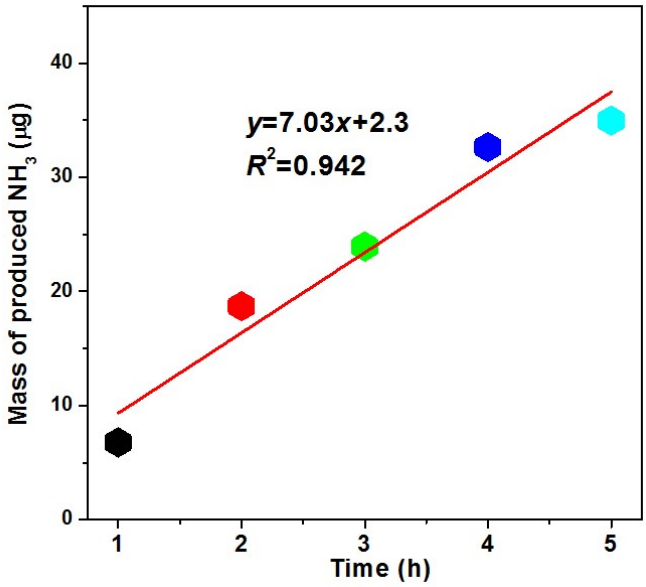

Fig. S7. Mass of produced NH_3 after NRR electrolysis at various times (1-5 h) on ZrB_2 NCs at -0.3 V.

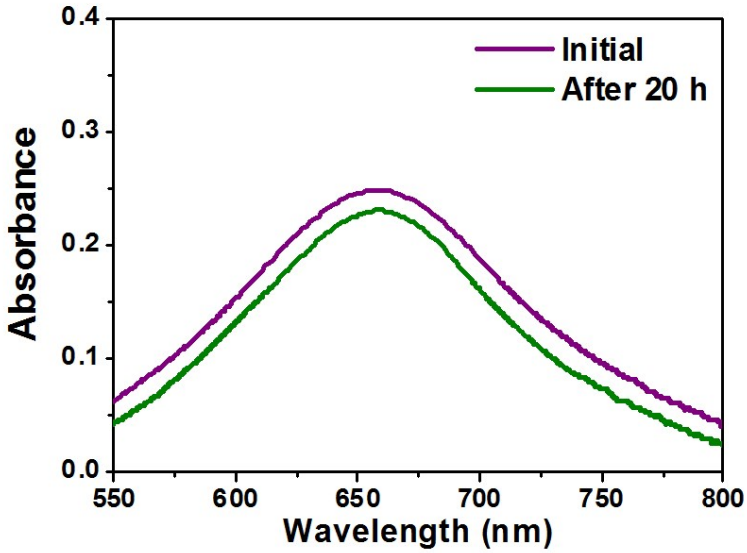

Fig. S8. UV-vis absorption spectra of the electrolytes for initial and post-NRR electrolysis (after 20 h) on ZrB_2 NCs at -0.3 V.

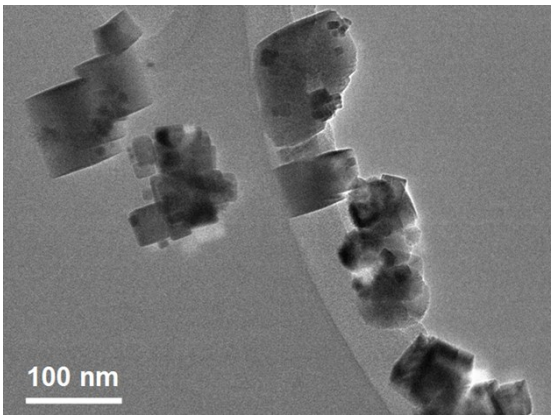

Fig. S9. TEM image of ZrB_2 NCs after stability test.

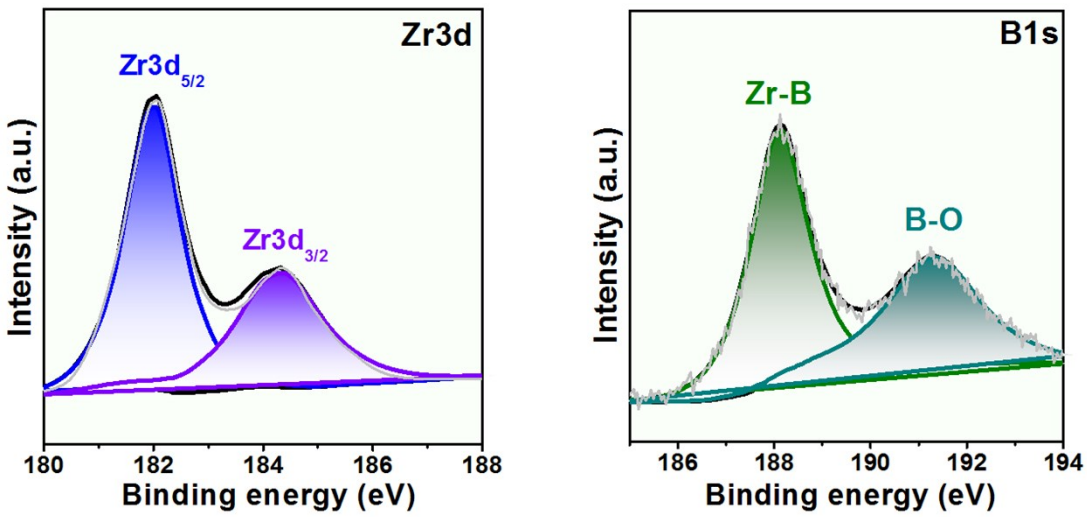

Fig. S10. XPS spectra of ZrB_2 NCs after stability test. (a) Zr3d. (b) B1s.

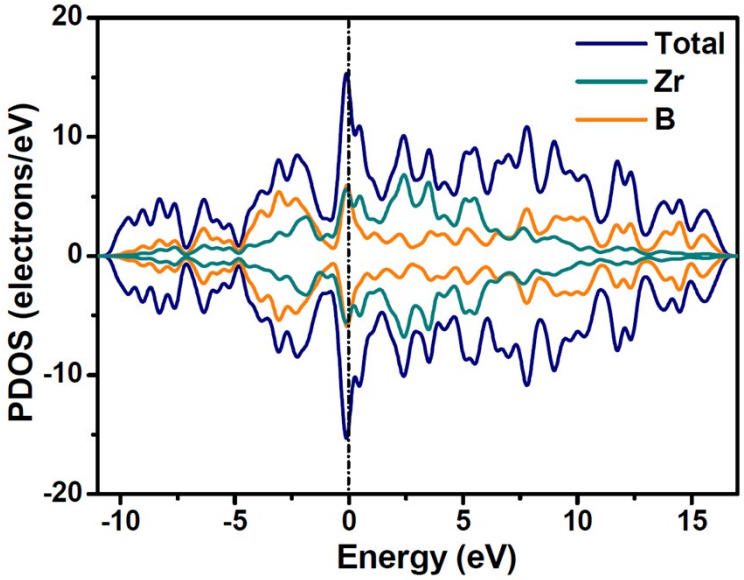

Fig. S11. Projected density of states (PDOS) of ZrB_2 (001).

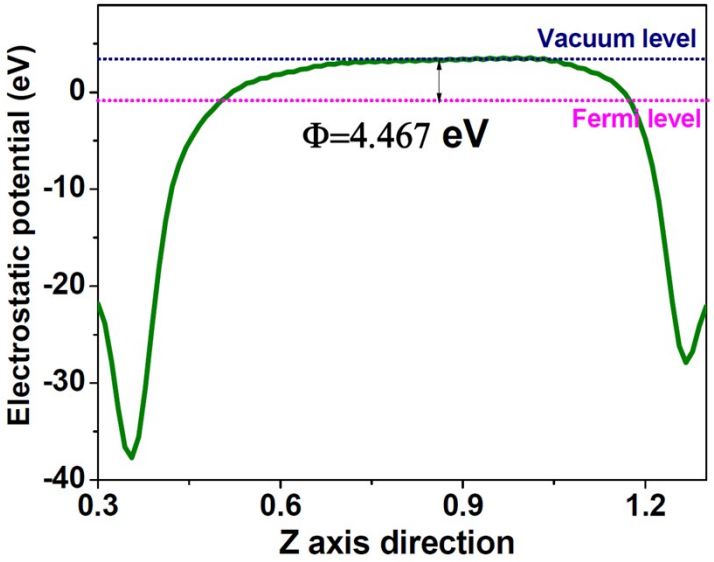

Fig. S12. Average potential profiles along c-axis direction for calculating the work function of ZrB_2 (001).

Table S1. Comparison of optimum NH_3 yield and Faradic efficiency (FE) for recently reported state-of-the-art NRR electrocatalysts at ambient conditions

Catalyst	Electrolyte	Determination method	Optimum Potential (V Vs RHE)	NH_3 yield	FE (%)	Ref.
MnO particles	0.1 M Na_2SO_4	Indophenol blue method	-0.39	7.92 μg h^{-1} mg^{-1}	8.02	[10]
Mn_3O_4 nanocubes	0.1 M Na_2SO_4	Indophenol blue method	-0.8	11.6 μg h^{-1} mg^{-1}	3	[11]
La_2O_3 nanoplate	0.1 M Na_2SO_4	Indophenol blue method	-0.8	17.04 μg h^{-1} mg^{-1}	4.76	[12]
Y_2O_3 Nanosheet	0.1 M Na_2SO_4	Indophenol blue method	-0.9	1.06×10^{-10} mol s^{-1} cm^{-2}	2.53	[13]
B_4C nanosheet	0.1 M HCl	Indophenol blue method	-0.75	26.57 μg h^{-1} mg^{-1}	15.95	[14]
MoS_2 nanosheet	0.1 M Na_2SO_4	Indophenol blue method	-0.5	8.08×10^{-11} mol s^{-1} cm^{-2}	1.17	[15]
Defect-rich MoS_2 nanoflower	0.1 M Na_2SO_4	Indophenol blue method	-0.4	29.28 μg h^{-1} mg^{-1}	8.34	[16]
Au-TiO_2 sub-nanocluster	0.1 M HCl	Indophenol blue method	-0.2	21.4 μg h^{-1} mg^{-1}	8.11	[17]
Au nanorods	0.1 M KOH	Nessler's reagent method	-0.2	1.65 μg cm^{-2} h^{-1}	4.02	[18]
Mo_2C/C	0.5 M Li_2SO_4	Nessler's reagent method	-0.3	11.3 μg h^{-1} mg^{-1}	7.8	[19]
MXene	0.5 M Li_2SO_4	Nessler's reagent method	-0.1	4.7 μg cm^{-2} h^{-1}	5.78	[20]
Mosaic Bi nanosheets	0.1 M Na_2SO_4	Indophenol blue method	-0.8	13.23 μg h^{-1} mg^{-1}	10.46	[21]
Porous Au Film	0.1 M Na_2SO_4	Indophenol blue method	-0.2	9.42 μg cm^{-2} h^{-1}	13.36	[22]
B-doped graphene	0.05 M H_2SO_4	Indophenol blue method	-0.5	9.8 μg cm^{-2} h^{-1}	10.8	[23]
Boron nitride nanosheet	0.1 M HCl	Indophenol blue method	-0.75	22.4 μg h^{-1} mg^{-1}	4.7	[24]
Defect-rich fluorographene nanosheet	0.1 M Na_2SO_4	Indophenol blue method	-0.7	9.3 μg h^{-1} mg^{-1}	4.2	[25]
ZrB_2 NCs	**0.5 M $LiClO_4$**	**Indophenol blue method**	**-0.3**	**37.7 μg h^{-1} mg^{-1}**	**18.2**	**This work**

Supplementary references

[1]. Q. Li, X. Zou, X. Ai, H. Chen, L. Sun and X. Zou, *Adv. Energy. Mater.*, 2019, **9**, 1803369.

[2]. K. Chu, W. Gu, Q. Li, Y. Liu, Y. Tian and W. Liu, *J. Energy Chem.*, 2021, **53**, 82-89.

[3]. K. Chu, Y. P. Liu, Y. B. Li, Y. L. Guo and Y. Tian, *ACS Appl. Mater. Inter.*, 2020, **12**, 7081-7090.

[4]. K. Chu, Y. Liu, Y. Li, Y. Guo, Y. Tian and H. Zhang, *Appl. Catal. B*, 2020, **264**, 118525.

[5]. D. Zhu, L. Zhang, R. E. Ruther and R. J. Hamers, *Nat. Mater.*, 2013, **12**, 836.

[6]. G. W. Watt and J. D. Chrisp, *Anal. Chem.*, 1952, **24**, 2006-2008.

[7]. B. Hu, M. Hu, L. C. Seefeldt and T. L. Liu, *ACS Energy Lett.*, 2019, **4**, 1053-1054.

[8]. S. J. Clark, M. D. Segall, C. J. Pickard, P. J. Hasnip, M. I. J. Probert, K. Refson and M. C. Payne, *Z. Kristallogr.*, 2005, **220**, 567-570.

[9]. A. A. Peterson, *Energy Environ. Sci.*, 2010, **3**, 1311-1315.

[10]. Z. Wang, F. Gong, L. Zhang, R. Wang, L. Ji, Q. Liu, Y. Luo, H. Guo, Y. Li, P. Gao, X. Shi, B. Li, B. Tang and X. Sun, *Adv. Sci.*, 2018, 1801182.

[11]. X. Wu, L. Xia, Y. Wang, W. Lu, Q. Liu, X. Shi and X. Sun, *Small*, 2018, **14**, 1803111.

[12]. B. Xu, Z. Liu, W. Qiu, Q. Liu, X. Sun, G. Cui, Y. Wu and X. Xiong, *Electrochim. Acta*, 2018, **298**, 106-111.

[13]. X. Li, L. Li, X. Ren, D. Wu, Y. Zhang, H. Ma, X. Sun, B. Du, Q. Wei and B. Li, *Ind. Eng. Chem. Res.*, 2018, **57**, 16622-16627.

[14]. W. Qiu, X.-Y. Xie, J. Qiu, W.-H. Fang, R. Liang, X. Ren, X. Ji, G. Cui, A. M. Asiri and G. Cui, *Nat. Commun.*, 2018, **9**, 3485.

[15]. L. Zhang, X. Ji, X. Ren, Y. Ma, X. Shi, Z. Tian, A. M. Asiri, L. Chen, B. Tang and X. Sun, *Adv. Mater.*, 2018, **30**, 1800191.

[16]. X. Li, T. Li, Y. Ma, Q. Wei, W. Qiu, H. Guo, X. Shi, P. Zhang, A. M. Asiri and L. Chen, *Adv. Energy. Mater.*, 2018, **8**, 1801357.

[17]. M. M. Shi, D. Bao, B. R. Wulan, Y. H. Li, Y. F. Zhang, J. M. Yan and Q. Jiang, *Adv. Mater.*, 2017, **29**, 1606550.

[18]. D. Bao, Q. Zhang, F. L. Meng, H. X. Zhong, M. M. Shi, Y. Zhang, J. M. Yan, Q. Jiang and X. B. Zhang, *Adv. Mater.*, 2017, **29**, 1604799.

[19]. H. Cheng, L. X. Ding, G. F. Chen, L. Zhang, J. Xue and H. Wang, *Adv. Mater.*, 2018, **30**, 1803694.

[20]. Y. R. Luo, G. F. Chen, L. Ding, X. Z. Chen, L. X. Ding and H. H. Wang, *Joule*, 2019, **3**, 279-289.

[21]. L. Li, C. Tang, B. Xia, H. Jin, Y. Zheng and S.-Z. Qiao, *ACS Catal.*, 2019, **9**, 2902-2908.

[22]. H. Wang, H. Yu, Z. Wang, Y. Li, Y. Xu, X. Li, H. Xue and L. Wang, *Small*, 2019, **15**, 1804769.

[23]. X. Yu, P. Han, Z. Wei, L. Huang, Z. Gu, S. Peng, J. Ma and G. Zheng, *Joule*, 2018, **2**, 1610-1622.

[24]. Y. Zhang, H. Du, Y. Ma, L. Ji, H. Guo, Z. Tian, H. Chen, H. Huang, G. Cui, A. M. Asiri, F. Qu, L. Chen and X. Sun, *Nano Res.*, 2019, **12**, 919-924.

[25]. J. Zhao, J. Yang, L. Ji, H. Wang, H. Chen, Z. Niu, Q. Liu, T. Li, G. Cui and X. Sun, *Chem. Commun.*, 2019, **55**, 4266-4269.